Structural and Dynamical Properties of an $LiCl \cdot 3H_2O$ Solution

Y. Tamura

Department of Electronic Chemistry, Tokyo Institut of Technology, Nagatsuta, Midori-ku, Yokohama 227, Japan

K. Tanaka

The Institute of Physical and Chemical Research, Wako-shi, Saitama 351-01, Japan

E. Spohr, and K. Heinzinger

Max-Planck Institut für Chemie (Otto-Hahn-Institut), D-6500 Mainz, FRG

Z. Naturforsch. **43a**, 1103–1110 (1988); received September 23, 1988

An MD simulation of an 18.5 molal LiCl aqueous solution was performed with the flexible Bopp-Jancsó-Heinzinger model for water, ion-water pair potentials derived from ab initio calculations and the ion-ion interactions described by a potential of Born-Mayer-Huggins (BMH) type. The comparison with a simulation of the same system, where the ion-ion interactions were described by a (12-6) Lennard-Jones + Coulomb potential, demonstrates that such a change affects not only the ion-ion but also the ion-water radial distribution functions significantly, and that the results with the BMH potential conform better to X-ray results. The self-diffusion coefficients for water and the ions are found to be lower by almost one order of magnitude compared with dilute solutions, in good agreement with experimental results. The spectral densities of the hindered translational motions as well as those of the librations and the internal vibrations of the water molecules have been calculated from the simulations through the corresponding velocity autocorrelation functions.

I. Introduction

In a recent paper on the structure of an 18.5 molal LiCl solution a discrepancy was reported between the $Cl^- - Cl^-$ radial distribution function (RDF) obtained from a Molecular Dynamics (MD) simulation [1] and a neutron diffraction study by Copestake et al. [2]. The potentials used for the LiCl solution were the same as the ones employed in an MD simulation of a 13.9 molal solution, the results of which had led to satisfactory agreement with X-ray measurements [3].

In both simulations the ion-ion interactions were described by Lennard-Jones (LJ) spheres with an elementary charge in the center. The BJH model for water was employed [4], and the ion-water potentials were derived from ab initio calculations. At a concentration of 2.2 molal this LJ model for the ions together with the ST2 model for water has proved to be very useful for the description of the structural and dynamical properties of various alkali halide solutions (see e.g. [5]).

As the $Cl^- - Cl^-$ RDF has to be calculated from the neutron diffraction measurements by the second order difference method, which involves large statistical errors, some doubt remained on the accuracy of the experimental results. But the discrepancy mentioned above could just as well be caused by limitations of the potentials employed in the simulation. After the discrepancy was found in the $Cl^- - Cl^-$ RDF it seemed appropriate to check first the ion-ion potentials. Therefore, the LJ potentials were replaced by Born-Mayer-Huggins potentials with parameters as originally proposed by Tosi and Fumi [6] and modified by Okada et al. [7], which proved to lead to a good description of the structural and dynamical properties of various molten salts.

In the following section the ion-ion pair potentials are presented and details of the simulation are reported. In Sect. III the structural properties of the 18.5 molal LiCl solution are described by various RDFs. It is demonstrated how the change in the ion-ion potential affects the simulated structure of the solution. The dynamical properties are discussed on the basis of the self-diffusion coefficients, the hindered translational motions and the librations and internal vibrations of the water molecules. They have been calculated from the simulation through various autocorrelation functions.

Reprint requests to Dr. Y. Tamura, Max-Planck-Institut für Chemie, Saarstraße 23, D-6500 Mainz.

0932-0784 / 88 / 1200-1103 $ 01.30/0. – Please order a reprint rather than making your own copy.

II. Pair Potentials and Details of the Simulations

The Born-Mayer-Huggins (BMH) potentials employed in the simulation for the ion-ion interactions are usually written in the form

$$V_{ij} = z_i z_j e^2 r^{-1} + A_{ij} b \exp[(\sigma_i + \sigma_j - r)/\varrho] - C_{ij} r^{-6} - D_{ij} r^{-8}, \quad (1)$$

where $z_i e$ is the charge of the ion i, $b = 0.338 \cdot 10^{-19}$ J, $\sigma_{Li} = 0.816$ Å, $\sigma_{Cl} = 1.585$ Å [6] and $\varrho = 0.313$ Å [7]. A_{ij}, C_{ij}, and D_{ij} are given in Table 1. For the water-water interactions the BJH model was employed [4], and the ion-water potentials were derived from ab initio calculations and were the same as in previous simulations of highly concentrated LiCl solutions [1, 3].

The ion-ion pair potentials are shown in Fig. 1 and compared with the (12-6) LJ potentials with an elementary charge in the center as used in the previous simulation (dashed) [1, 3]. The differences between the two kinds of potential are very large at small distances and disappear beyond 4 Å, where even in $V_{ClCl}(r)$ only the Coulomb interaction remains.

The basic cube contained again 129 water molecules and 43 ions of each kind. With the experimental density of 1.275 g/cm^3 a sidelength of the cube of 17.55 Å resulted. The simulation extended over 30 000 time steps equivalent to a total elapsed time of 7.5 ps at an average temperature of 310 K without rescaling. Further details of the simulation can be found in [1, 3].

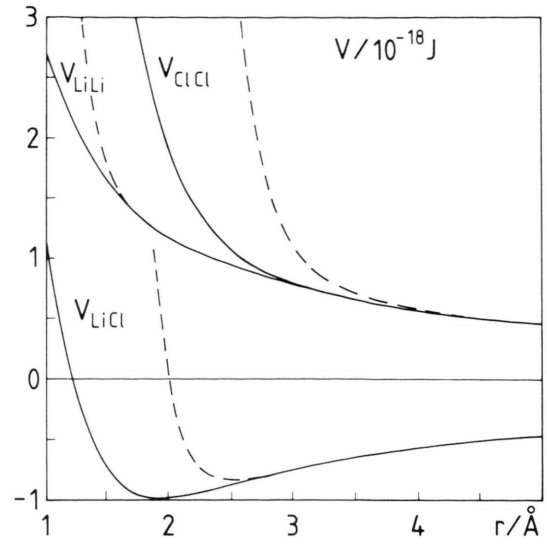

Fig. 1. Ion-ion pair potentials of Born-Mayer-Huggins type with parameters taken from [6, 7] (full) and of (12-6) Lennard-Jones type with an elementary charge in the center with the parameters taken from [3] (dashed).

Table 1. Parameters for the ion-ion potential as given in (1), taken from [7].

	Li–Li	Li–Cl	Cl–Cl
A	2.0	1.375	0.75
$C/10^{-19}$ JÅ^6	0.073	2.0	116.7
$D/10^{-19}$ JÅ^8	0.03	2.4	234.3

III. Results and Discussion

a) Radial Distribution Functions

The changes in the ion-ion potentials from LJ to BMH do not only cause changes in the ion-ion RDFs (Fig. 3) but also in the ion-water RDFs (Figure 2). While the positions of the first peaks in $g_{LiO}(r)$ and $g_{LiH}(r)$ remain unchanged the heights of the peaks decrease significantly, which is connected with a decrease of the hydration number of Li^+ by about 10% to 3.6. The first maximum in $g_{ClO}(r)$ is shifted by about 0.1 Å to larger distances without a change in height while the position of the first peak in $g_{ClH}(r)$ remains practically unchanged, but its height is significantly reduced. This reduction results in a decrease of the number of nearest hydrogen atoms around Cl^- by about 1 to a value of 4.

The changes in the water-water RDFs caused by the changes in the ion-ion potentials are rather small. Therefore, they are not depicted here. But the differences in the ion-ion RDFs are dramatic, as can be seen from Figure 3.

The smallest change occurs in $g_{LiLi}(r)$. The position of the first maximum is shifted for the BMH potential to a distance larger by about 0.2 Å, and the height is increased by about 10% relative to the LJ potential. While the position of the first peak at 3.2 Å corresponds to $2\,Li^+$ separated by a water molecule, the formation of a strong shoulder at about 4 Å seems to arise from configurations where $2\,Li^+$ are in contact with the same Cl^-. The number of these configurations is expected to increase with an increased tendency for contact ion pair formation.

This increase of contact ion pairs can be read from $n_{LiCl}(r)$ at the position of the first minimum in $g_{LiCl}(r)$ at around 3.5 Å and amounts to an average of about

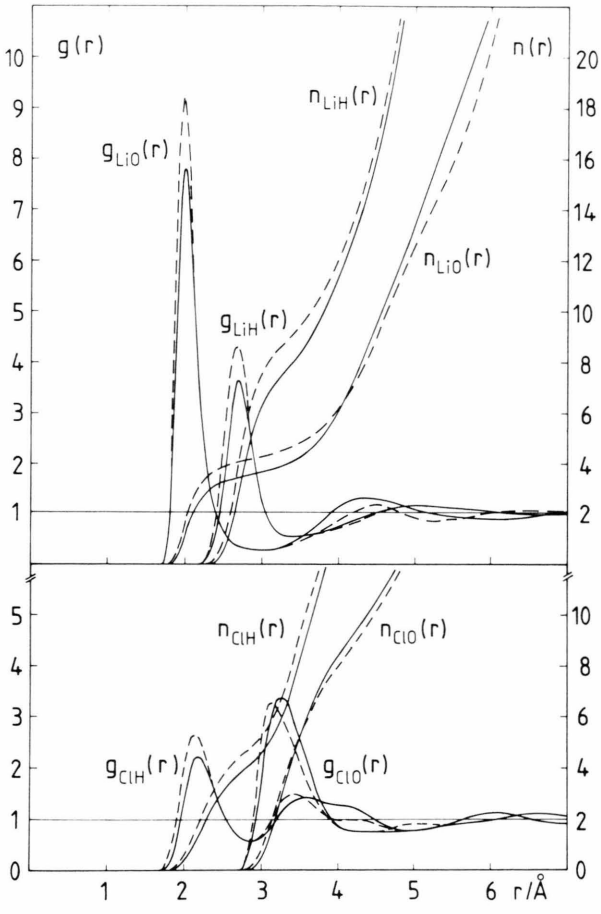

Fig. 2. Ion-oxygen and ion-hydrogen radial distribution functions and running integration numbers from MD simulations of an 18.5 molal LiCl solution with a Born-Mayer-Huggins (full) and a (12-6) Lennard-Jones (dashed) potential for the ion-ion interactions.

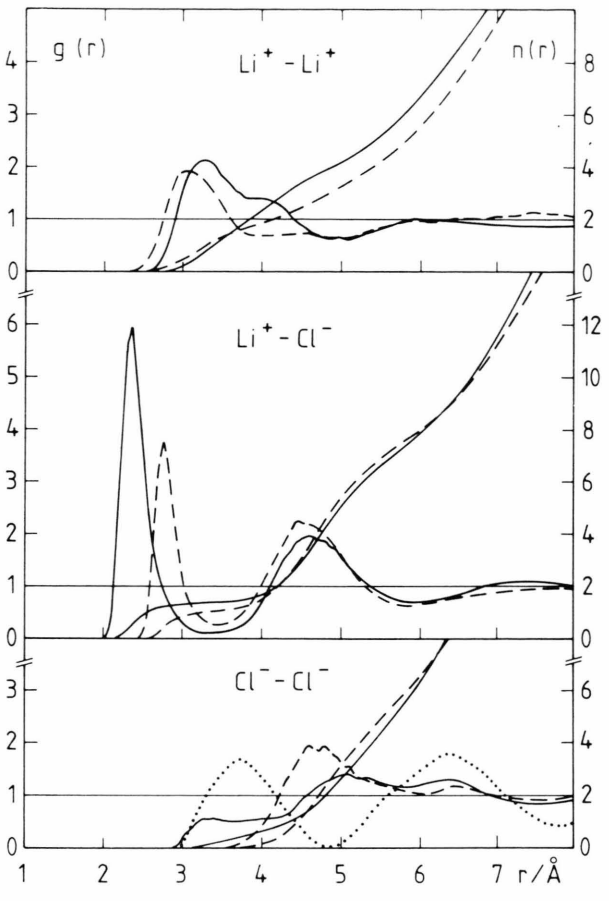

Fig. 3. Ion-ion radial distribution functions and running integration numbers from MD simulations of an 18.5 molal LiCl solution with a Born-Mayer-Huggins (full) and a Lennard-Jones (dashed) potential for the ion-ion interactions. The dotted line gives the result of a neutron diffraction study of a 14.9 molal LiCl solution with chloride isotope substitution [2].

1.5 Li^+ in contact with a Cl^- (Figure 3). The shift of the position of the first peak in $g_{LiCl}(r)$ by about 0.5 Å follows directly from the difference in the position of the potential minima for the BMH and the LJ potential as shown in Figure 1. The increase in the height of the first maximum is in keeping with the lower minimum of the BMH potential. The differences between the two $g_{LiCl}(r)$ become much smaller in the range of the second peak, as the differences between the two types of ion-ion potentials are restricted to distances smaller than 4 Å (Figure 1).

The $Cl^- - Cl^-$ RDF again strongly depends on the choice of the potential (Fig. 3). As a consequence of the much softer BMH potential relative to the LJ one (Fig. 1) the first peak in $g_{ClCl}(r)$ between 4.5–5 Å practically disappears and the $Cl^- - Cl^-$ RDF extends down to 3 Å, the distance of closest approach of two Cl^-. The dotted line results from the application of the second order difference method to neutron diffraction studies of a 14.9 molal aqueous LiCl solution with chloride isotope substitution by Copestake et al. [2]. With the change of the ion-ion potential from LJ to BMH type the discrepancy between simulation and experiment is reduced but still remains significant. As mentioned before [1], it seems to us very surprising that the experiment gives such a far ranging pronounced order of the chloride ions in the solution. It is very difficult to imagine a consistent set of ion-ion

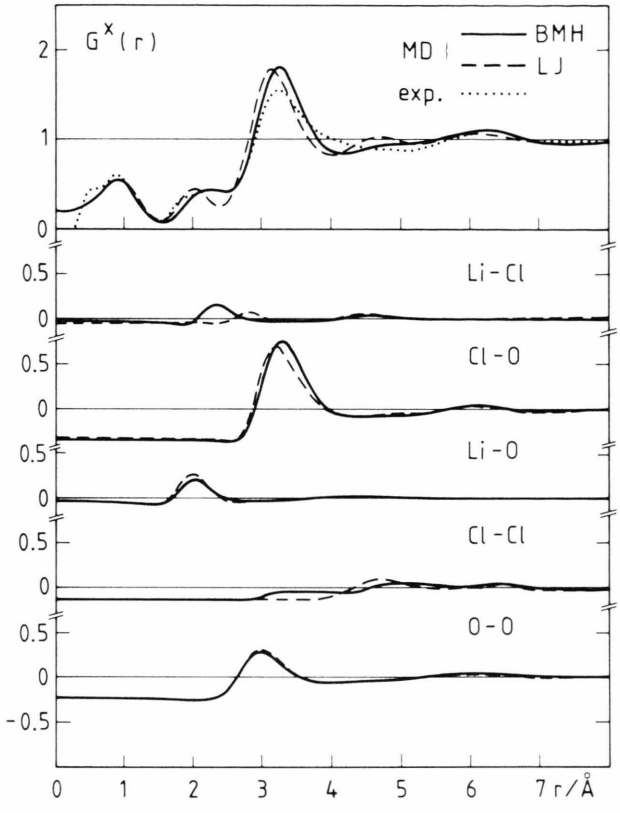

Fig. 4. Comparison of the total and selected partial X-ray weighted radial distribution functions from MD simulations of an 18.5 molal LiCl solution with a Born-Mayer-Huggins and a Lennard-Jones potential for the ion-ion interactions with the experimental one.

potentials which would lead to agreement with the experimental $Cl^- - Cl^-$ RDF. It is interesting to note that in spite of the discrepancies in $g_{ClCl}(r)$ the number of nearest neighbours is found to be nearly the same if all three RDFs are integrated to the minimum in the experimental RDF at 4.9 Å (see also discussion in [8]).

The total X-ray weighted RDFs from the two simulations with the different ion-ion potentials are compared in Fig. 4 with the experimental one [1]. In order to understand the improvement achieved with the BMH potential, the partial X-ray weighted RDFs – as far as they contribute significantly to the distinct part of the total RDF – are shown, too. The two main improvements follow from changes in the $Li^+ - Cl^-$ and $Cl^- - O$ RDFs. The shift in the position and the increase in the height of the first maximum in $g_{LiCl}(r)$ is responsible for the disappearance of the discrepancy in $G^x(r)$ at 2.4 Å. The unexpected strong effect of the change in the ion-ion potential on the position of the first peak in $g_{ClO}(r)$ corrects partly the second important discrepancy. There remains a difference in the heights of the main peak in $G^x(r)$ which also extends to larger distances in the experimental curve. It is not quite clear what the reason is for the remaining difference. Part of it might have to be attributed to difficulties with the Fourier transformation resulting from the limited range in k-space accessible by the experiment.

Neutron diffraction studies with chloride isotope substitution have been performed for a 14.9 molal LiCl solution [2] and others with lithium isotope substitution for a 27.7 molal LiCl solution at a temperature of 403 K [9]. Because of the strong differences in concentration a direct comparison of the simulated radial distribution or structure functions with the experimental ones is not possible. A rescaling of the data from the simulation to the concentrations used in the experiments seems not to be warranted as this can be done reliably only if the various partial distribution or structure functions involved do not change with concentration, which is not the case here. Therefore, a more detailed search for the reason of the remaining discrepancy between experiment and simulation cannot be performed now.

The orientations of the first neighbour water molecules relative to the cations and the anions do not change significantly with the change of the ion-ion potentials. They are, therefore, not depicted here.

b) Self-Diffusion Coefficients

The self-diffusion coefficients for Li^+, Cl^- and H_2O have been calculated from the mean square displacement and from the Green-Kubo relation via the velocity autocorrelation function. Both methods are mathematically identical and lead to the same result. The statistical uncertainty is relatively high as the self-diffusion coefficients in this highly concentrated solution are smaller by almost an order of magnitude when compared with dilute solutions. The results are compared in Table 2 with experimental data. The good agreement indicates that the potentials used in this simulation describe satisfactorily not only the structural but also the dynamical properties of the highly concentrated solution.

In dilute electrolyte solutions the self-diffusion coefficients and other dynamical properties are usually calculated from the simulation separately for the three

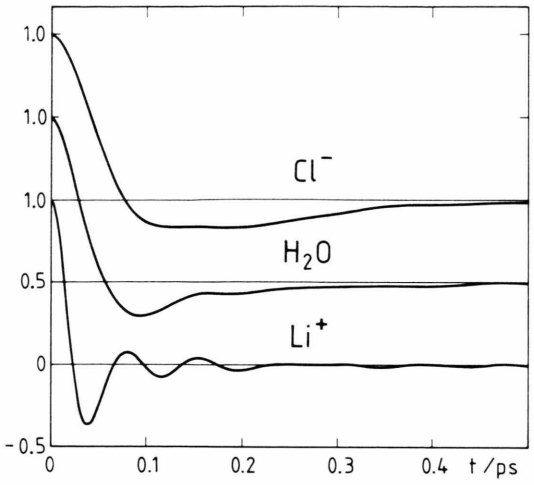

Fig. 5. Normalized velocity autocorrelation functions for Li^+, Cl^-, and water (center-of-mass) from an MD simulation of an 18.5 molal LiCl solution.

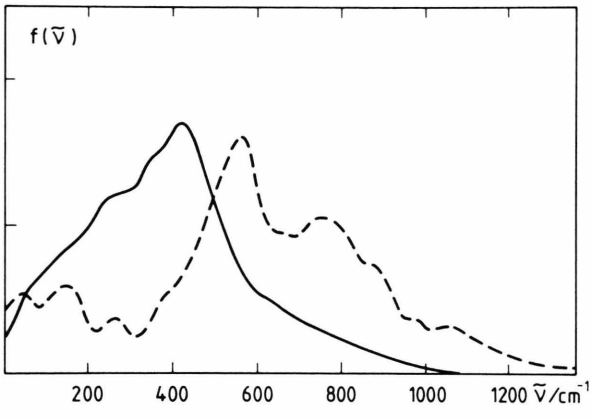

Fig. 6. Comparison of the spectral densities of the hindered translational motions of Li^+ from simulations of an 18.5 molal LiCl (full) and a 2.2 molal LiI [14] solution.

Table 2. Self-diffusion coefficients for water and the ions in an 18.5 molal LiCl solution at 310 K from the simulation with the BMH potential and experiment [10] in units of 10^{-5} cm^2/s. The statistical uncertainty of the MD values is estimated to be about 25%.

	Li^+	Cl^-	H_2O
MD	0.20	0.17	0.35
Experimental[a]	0.21	0.21	0.41
	0.20	0.20	0.34

[a] The experimental data in [10] have been measured at 298.2 K. They have been extrapolated here either according to the temperature dependence measured for a 15 molal LiCl solution (upper row) [11] or for the viscosities using the Stokes-Einstein relationship [12].

water subsystems – bulk water, hydration water of the cation and of the anion – in order to understand the single ion effect (see e.g. [13]). As at the concentration investigated here each water molecule belongs to the hydration shell of at least one cation and one anion, such a separate evaluation is not warranted.

c) Hindered Translational Motions

The velocity autocorrelation functions (acf) for Li^+, Cl^-, and H_2O (center-of-mass) are shown in Figure 5. In order to demonstrate the differences between the three acfs they are drawn only up to 0.5 ps, a correlation length which is not sufficient to calculate the self-diffusion coefficients as the acfs have not yet decayed to zero. These differences become more obvious and can be discussed more easily when the Fourier transforms of the acfs are compared, which gives the spectral densities of the hindered translational motions for Li^+, Cl^- and H_2O. They are shown in Fig. 6 for Li^+ and in Fig. 7 for Cl^- and H_2O.

Extended simulations for dilute aqueous LiCl solutions with the same potentials as employed here have not been performed. Therefore, the spectral density of the hindered translational motions of Li^+ in the 18.5 molal LiCl solution is compared in Fig. 6 with the one calculated from the simulation of a 2.2 molal LiI solution with the ST2 model for water, where the ions are modelled as Lennard-Jones spheres with an elementary charge at the center [14]. These differences in the potentials are not expected to mask significantly the changes caused by a strong increase in concentration. It can be read from Fig. 6 that at the high concentration the shoulder at about 800 cm^{-1} has disappeared, and the main peak is shifted to the red by more than one hundred wavenumbers. The relatively high frequencies found for the translational motions of Li^+ at low concentration were explained before by the strong interactions of Li^+ within the cage of its six firmly attached water molecules together with the coupling of the librations of the hydration shell water molecules with the translations of the ion [14]. In keeping with this explanation in the highly concentrated solution the hydration shell cage breaks down by the contact ion pair formation, the forces become asymmetric and the coupling is strongly reduced, resulting in the red-shift found.

The spectral densities of the hindered translational motions of Cl^- and H_2O in the 18.5 molal LiCl solu-

tion are compared in Fig. 7 with those calculated from the simulation of a 1.1 molal $SrCl_2$ solution, where also the BJH model for water was employed and the Cl^--water potentials were the same as here. Through this comparison the effect of concentration becomes obvious, as in the dilute case the hydration shell of Cl^- is not influenced by the cations and bulk water is in all its properties very similar to that of pure water [15].

The increase in concentration leads for Cl^- to a blueshift of about 25 cm^{-1} in the maximum of spectral density of the hindered translations and a broadening. This shift to higher frequencies has to be attributed to the stronger interaction of Cl^- ions as a consequence of contact ion pair formation. Different from the Li^+ case, a well defined hydration shell does not exist around Cl^- which could break down.

In pure water the hindered translational motions around 50 cm^{-1} are usually attributed to hydrogen bond bending and the broad peak around 175 cm^{-1} to O–O stretching motions (dashed curve in Fig. 7). At the high concentration this assignment is no longer possible, the spectral density found here is quite similar to that for the hydration shell water molecules of Li^+ in dilute solutions [14]. Thus, it can be concluded that the lithium ions mainly determine the translational behaviour of water in the highly concentrated LiCl solution.

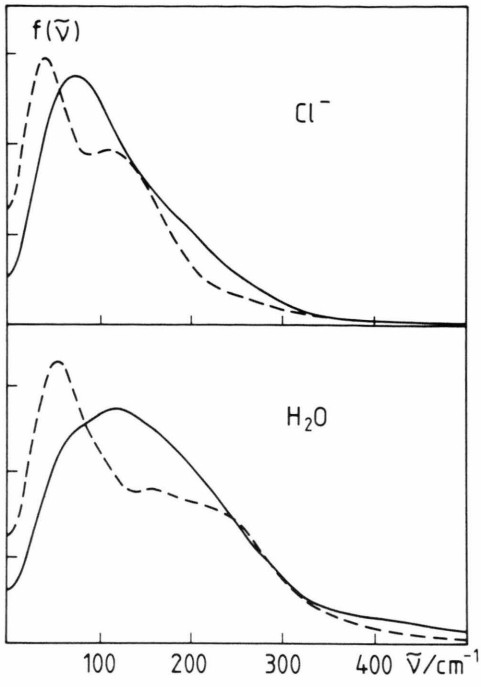

Fig. 7. Comparison of the spectral densities of the hindered translational motions of Cl^- and water from simulations of an 18.5 molal LiCl (full) and a 1.1 molal $SrCl_2$ solution [15].

d) Librational Motions

The angular velocity autocorrelation functions have been calculated from the simulation separately for the rotations around the three main axes of the water molecules and are depicted in Figure 8. Their respective Fourier transforms – the spectral densities of the librations – are compared in Fig. 9 with the ones for pure water [16], where the differences in the positions of the maxima result from the different moments of inertia around the axes.

It can be read from Fig. 9 that the ions in the 18.5 molal LiCl solution cause a blueshift of the librations of the water molecules around the x- and y-axes of about 150 cm^{-1} while the libration around the z-axis remains practically unchanged. This result is in accordance with the orientation of the water molecules relative to the two ions. There exists a strong preference for a trigonal orientation relative to Li^+ (the dipole moment of the water molecule points away from the center of the ion) while a slight preference exists for the formation of a linear hydrogen bond

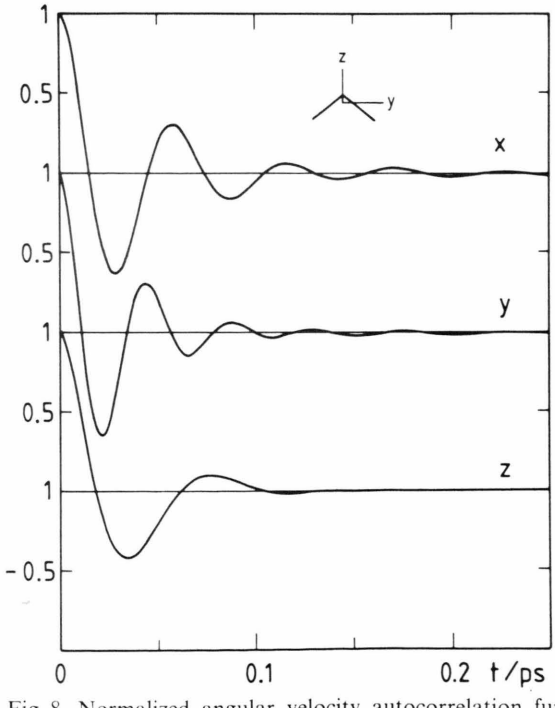

Fig. 8. Normalized angular velocity autocorrelation functions of the water molecules in an 18.5 molal LiCl solution, calculated separately for the three components in a molecule fixed coordinate system as defined in the insertion.

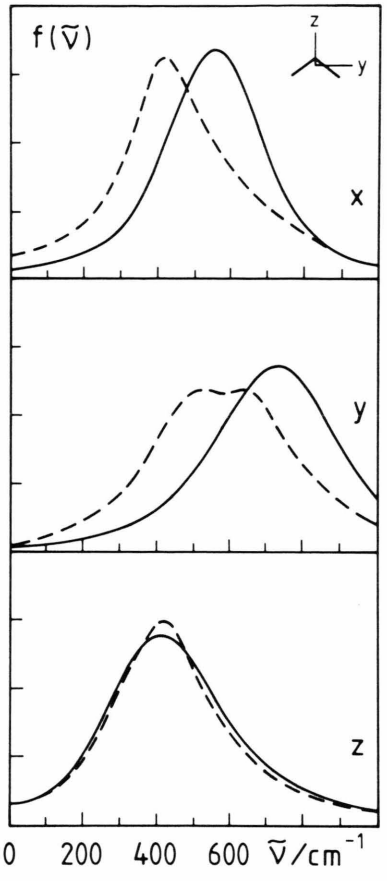

Fig. 9. Comparison of the spectral densities of the librations around the three main axes of the water molecule as calculated from simulations of 18.5 molal LiCl solutions (full) and of pure BJH water (dashed) [16]. The molecule fixed coordinate system is defined in the insertion.

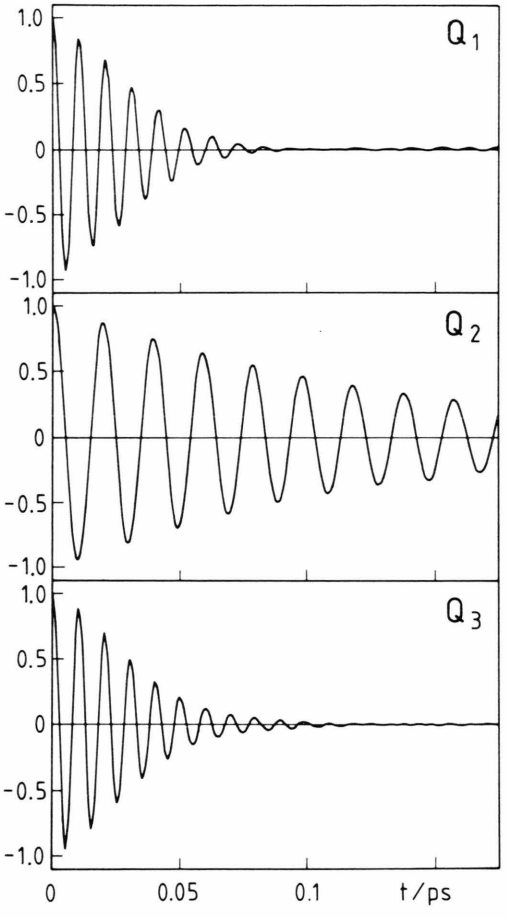

Fig. 10. Velocity autocorrelation functions for the three vibrational modes of the water molecules in an 18.5 molal LiCl solution. Q_1, Q_2, and Q_3 denote the symmetric stretching, bending, and asymmetric stretching modes, respectively.

with Cl^- [1]. These preferential orientations did not change significantly with the change in the ion-ion potential from the LJ to the BMH type and are, therefore, not depicted here.

It can be visualized easily that in the case of a trigonal orientation of the hydrating molecules Li^+ does not influence the rotation around the dipole axis (z-axis). As it has been found from the simulation of the 1.1 molal $SrCl_2$ solution that the spectral density of the librations for the water molecules in the hydration shell of Cl^- are not significantly different from that of bulk water [15], it is easily understood that even in the highly concentrated LiCl solution a frequency shift of the librations around the z-axis relative to pure water has not been found. Different from the z-axis, the librational motions around the other two axes of the water molecule are significantly hindered by the strong ion-water interactions and, therefore, a remarkable blueshift relative to pure water results from the simulation.

e) Intramolecular Geometry and Vibrations

The combined effect of Li^+ and Cl^- on the water molecule geometry leads in this highly concentrated solution to an average O–H distance of 0.9879 Å and to an average HOH angle of 97.3°. These values have to be compared with the corresponding ones from a simulation of pure water of 0.9755 Å and 100.8°, respectively. From this geometry and the charge dis-

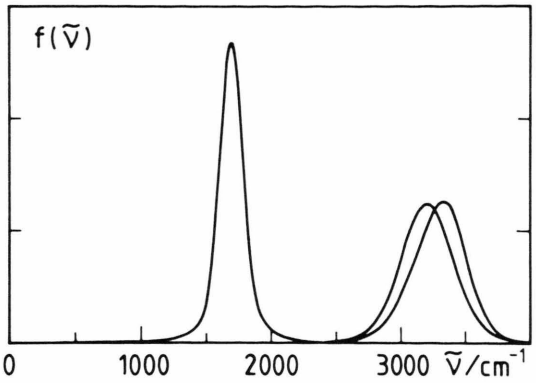

Fig. 11. Spectral densities of the intramolecular vibrations of the water molecules as calculated from a simulation of an 18.5 molal LiCl solution.

tribution a dipole moment of 2.09 D results, which is about 5% larger than that found for pure BJH water [4].

In Fig. 10 the velocity autocorrelation functions are shown separately for the three vibrational modes of the water molecules in the 18.5 molal LiCl solution. They have been calculated from the hydrogen atom velocities through a scheme which is described in the Appendix of [15]. The Fourier transforms of these velocity autocorrelation functions are shown in Figure 11. The maxima in the spectral densities of the bending, symmetric and asymmetric O–H stretching vibrations appear at 1700, 3210, and 3325 cm^{-1}, respectively. The comparison with the corresponding values from the simulation of pure BJH water [16] shows that in the limits of statistical uncertainty the frequency of the bending vibration does not change while for both stretching vibrations a redshift of about 260 cm^{-1} is found for the concentrated LiCl solution. This shift is in keeping with the increased intramolecular O–H distance if the empirical relationship of about 20 000 $cm^{-1}/Å$ is applied [17].

Acknowledgement

Financial support by Deutsche Forschungsgemeinschaft is gratefully acknowledged.

[1] K. Tanaka, N. Ogita, Y. Tamura, I. Okada, H. Ohtaki, G. Pálinkás, E. Spohr, and K. Heinzinger, Z. Naturforsch. **42a**, 24 (1987).
[2] A. P. Copestake, G. W. Neilson, and J. E. Enderby, J. Phys. C: Solid State Phys. **18**, 4211 (1985).
[3] P. Bopp, I. Okada, H. Ohtaki, and K. Heinzinger, Z. Naturforsch. **40a**, 116 (1985).
[4] P. Bopp, G. Jancsó, and K. Heinzinger, Chem Phys. Lett. **98**, 129 (1983).
[5] K. Heinzinger, Pure Appl. Chem. **57**, 1031 (1985).
[6] M. P. Tosi and F. G. Fumi, J. Phys. Chem. Solids **25**, 31 (1964).
[7] I. Okada, H. Okano, H. Ohtaki, and R. Takagi, Chem. Phys. Lett. **100**, 436 (1983).
[8] J. E. Enderby, S. Cummings, G. J. Herdman, G. W. Neilson, P. S. Salmon, and N. Skipper, J. Phys. Chem. **91**, 5851 (1987).
[9] K. Ichikawa, Y. Kameda, T. Matsumoto, and M. Misawa, J. Phys. C: Solid State Phys. **17**, L 725 (1984).
[10] K. Tanaka and M. Nomura, J. Chem. Soc. Faraday Trans. I **83**, 1779 (1987).
[11] M. Fontanella, N. Micali, and F. Wanderlingh, Phys. Chem. Liquids **15**, 283 (1986).
[12] K. Tanaka, unpublished data.
[13] Gy. I. Szász, K. Heinzinger, and W. O. Riede, Ber. Bunsenges. Phys. Chem. **85**, 1056 (1981).
[14] Gy. I. Szász and K. Heinzinger, J. Chem. Phys. **79**, 3467 (1983).
[15] E. Spohr, G. Pálinkás, K. Heinzinger, P. Bopp, and M. M. Probst, J. Phys. Chem., in press.
[16] P. Bopp, Habilitationsschrift, Darmstadt 1988.
[17] S. I. La Placa, W. C. Hamilton, B. Kamb, and A. Prakash, J. Chem. Phys. **58**, 567 (1973).